The Oxidative Folding Rate of Bovine Pancreatic Ribonuclease Is Enhanced by a Covalently Attached Oligosaccharide†

Guoqiang Xu, Mahesh Narayan, and Harold A. Scheraga*

Baker Laboratory of Chemistry and Chemical Biology, Cornell University, Ithaca, New York 14853-1301

Received April 15, 2005; Revised Manuscript Received May 21, 2005

ABSTRACT: Bovine pancreatic ribonuclease B (RNase B) differs from RNase A by the presence of an oligosaccharide moiety covalently attached to Asn 34. Oxidative folding studies of RNase B were carried out at different temperatures using DTT^{ox} as the oxidizing agent, and the results were compared with those for RNase A. The oxidative folding rates of RNase B are between 1.7 and 1.3 times faster than those of RNase A at the temperatures that were investigated. The folding pathways of RNase B were determined to be similar to those of RNase A in that two structured intermediates, each lacking one native disulfide bond, were found to populate the regeneration pathways at 25 °C and pH 8.3. The thermodynamic stabilities of these two glycosylated intermediates, and their rates of formation from their unstructured precursors in the rate-determining step, were found to be higher than those of their unglycosylated counterparts from RNase A. Thus, the underlying cause for the faster rate of oxidative regeneration of native RNase B appears to be both thermodynamic and kinetic due to the higher stability, and faster rate of formation, of the intermediates of RNase B compared to those of RNase A.

The amino acid sequence of bovine pancreatic ribonuclease B (RNase B)[1] is identical to that of RNase A. An oligosaccharide moiety attached to Asn 34 through a single N-glycosylation site distinguishes RNase B from the defining member (RNase A) of the family of pancreatic RNases (*1*−*3*). Nevertheless, a comparison of the structures of the two proteins (*4*, *5*) revealed no significant differences between them, suggesting that the oligosaccharide moiety has no strong influence on the static protein conformation (*5*).

The RNase B protein occurs as a mixture of five glycoforms (isoforms), denoted as $Man_{5-9}GlcNAc_2$-RNase with five to nine mannoses in the oligosaccharide side chain (*6*, *7*). In general, oligosaccharides are known to stabilize proteins (*7*−*9*), increase their solubility in aqueous solutions (*10*), and facilitate the conformational folding and assembly of nascent chains (*11*, *12*). Furthermore, amide−proton exchange rate measurements of RNase B indicate that the presence of the oligosaccharide chain affects the solvent accessibility of many regions of the peptide backbone, both in the vicinity of and at sites remote from the glycosylation site (*6*, *8*).

N-Glycosylation is a cotranslational event in the formation of several proteins with the attachment of the oligosaccharide occurring prior to the conformational folding of the nascent polypeptide chain to form its tertiary structure (*13*, *14*). In vitro studies on RNase A indicate that it cannot be glycosylated to form RNase B unless its native structure is disrupted (*15*). Therefore, the effect of the oligosaccharide moiety on the oxidative folding pathway and kinetics of regeneration of bovine pancreatic ribonucleases is of interest.

Previous experiments have demonstrated that the rates of conformational refolding of disulfide-intact RNase A and B from the GdnHCl-denatured states are similar, and proceed through a two-state mechanism, indicating that the oligosaccharide has no effect on the conformational folding mechanism of bovine pancreatic ribonucleases (*16*). The oxidative refolding of the two ribonucleases, studied by both air oxidation (*17*) and a metal ion-catalyzed air oxidation (*18*), indicated that the recovery of enzymatic activity is faster for RNase B than for RNase A from their fully reduced forms (*17*, *18*).

Although the studies described above shed light on the overall folding kinetics of RNase B, a detailed understanding of the influence of the oligosaccharide on the oxidative regeneration pathways and their kinetics is still lacking because measurement of enzymatic activity as a test for completion of folding [used in previous studies (*17*, *18*)] can be misleading given that nativelike intermediates can be enzymatically active (*19*−*22*). Furthermore, the regeneration pathway of RNase B has yet to be determined and compared with its unglycosylated counterpart which oxidatively folds through two major three-disulfide-containing nativelike

† This work was supported by the National Institute of General Medical Sciences of the National Institutes of Health (Grant GM-24893).

* To whom correspondence should be addressed. Telephone: (607) 255-4034. Fax: (607) 254-4700. E-mail: has5@cornell.edu.

[1] Abbreviations: RNase A and RNase B, bovine pancreatic ribonuclease A and B, respectively; N and R, native and fully reduced proteins, respectively; (*x*−*y*) disulfide bond, disulfide bond formed between cysteines *x* and *y*; des [*x*−*y*], structured intermediate of RNase A or RNase B having all native disulfide bonds but lacking the (*x*−*y*) disulfide bond; *n*S, unstructured intermediate of ribonuclease having *n* disulfide bonds; 3S*, (structured) nativelike species having three native disulfide bonds; AEMTS, 2-amino ethylmethanethiosulfonate; DTT^{ox} and DTT^{red}, oxidized and reduced dithiothreitol, respectively; EDTA, ethylenediaminetetraacetic acid; Tris-HCl, tris(hydroxymethyl)aminomethane hydrochloride; GdnHCl, guanidine hydrochloride; HEPES, *N*-(2-hydroxyethyl)piperazine-*N*′-2-ethanesulfonic acid; HPLC, high-performance liquid chromatography; ESI/FTMS, electrospray ionization/Fourier transform mass spectrometry.

10.1021/bi0506932 CCC: $30.25
Published on Web 06/18/2005

intermediates, des [40−95] and des [65−72], that are formed in the rate-limiting step (*23*).

From a practical standpoint, it is difficult to separate individual RNase B carbohydrate isoforms from one another using traditional protein purification methods. In a previous study of the reductive unfolding pathways of RNase B (*24*), we were able to study the reductive unfolding pathways of all five carbohydrate isoforms of RNase B simultaneously using ESI/FTMS to differentiate each isoform species from the other four. Here, we studied the oxidative regeneration of a mixture of RNase B isoforms using high-performance liquid chromatography (HPLC), which has also been applied previously, in part, to study the reductive unfolding pathways of RNase B (*24*).

MATERIALS AND METHODS

Materials. RNase A and B were purchased from Sigma. RNase A was purified according to the method described previously (*25*). RNase B was purified further with a strong cation-exchange (SCX) HPLC system (Rainin Hydropore 5-SCX column) to remove the unglycosylated protein as described elsewhere (*24*). The absence of RNase A and the presence of all five isoforms of RNase B ($Man_{5-9}GlcNAc_2$) were confirmed by mass spectrometry (*24*). AEMTS (greater than 99% pure) was purchased from Anatrace. Oxidized dithiothreitol (DTT^{ox}) and reduced dithiothreitol (DTT^{red}) were obtained from Sigma and used without further purification. All other chemicals were of the highest grade commercially available.

Preparation of Fully Reduced RNase B. Purified native RNase B was reduced by incubating the protein in a buffer containing 100 mM DTT^{red} and 6 M GdnHCl (100 mM Tris-HCl, 1 mM EDTA, pH 8.3, 25 °C). After incubation for 3 h, the pH of the solution was lowered to 3 by addition of glacial acetic acid. The reduced protein was desalted (and DTT^{red} was removed) on a reversed-phase HPLC column (C-18) and lyophilized to remove the organic solvent and water. Lyophilized reduced protein was dissolved in a dilute acetic acid solution (pH 3.7) to obtain a stock solution (5.0 mg/mL) and was stored at −20 °C. Reduced RNase A was prepared by using the same procedure.

Oxidative Folding of RNase B. Oxidative folding of RNase B was carried out at three different temperatures, 15, 25, and 37 °C, by incubating 0.5 mg/mL (33 μM) reduced protein in a buffer of 100 mM DTT^{ox} (pH 8.3, 100 mM Tris-HCl, 1 mM EDTA). No DTT^{red} was present in the original oxidation buffer, but DTT^{red} accumulated during the oxidation reaction. Aliquots of 200 μL were withdrawn at different times after the initiation of oxidative folding, and any free thiols were blocked by an excess amount of AEMTS (final concentration of 50 mM, pH 8.3, 100 mM Tris-HCl and 1 mM EDTA). Five minutes after the addition of the AEMTS, the pH of the solution was lowered to 3 by addition of 20 μL of glacial acetic acid. All samples were desalted on a Hi-Trap G25 column by exchange against a 0.2% acetic acid solution before analysis using cation-exchange HPLC.

Prior to the addition of AEMTS which blocks any free thiols, some samples were subjected to a reduction pulse (5 mM DTT^{red} at pH 8.3 for 2 min) which results in the reduction of all unstructured species to the fully reduced protein (R), a procedure that has been used successfully to identify and isolate structured species in the oxidative folding of RNase A (*26*). To compare the regeneration profile of RNase B with that of RNase A, all experiments described above were also carried out with RNase A under similar conditions.

Isolation of Two AEMTS-Blocked Structured Intermediates (des species) from the RNase B Folding Mixture. Some samples that had been subjected to a reduction pulse during the oxidative folding at 25 °C and blocked with AEMTS were used to collect the two structured AEMTS-blocked intermediates using cation-exchange HPLC (to separate them from native and fully reduced species). The structured intermediates were desalted by reversed-phase HPLC prior to lyophilization. Their identity was established by comparing their elution times with those of intermediates identified in reductive unfolding studies of RNase B (*24*).

Determination of GdnHCl Denaturation Curves of Two AEMTS-Blocked Des RNase B Intermediates. Isolated AEMTS-blocked structured des intermediates (1 mg each) were separately dissolved in 200 μL of dilute acetic acid (pH 3.7) prior to addition into an optical cell containing 1.8 mL of Tris buffer (100 mM Tris-HCl, 1 mM EDTA, pH 8.3, 25 °C). The absorbance of the protein was measured on a Cary 100 spectrophotometer at 287 nm (25 °C). Small aliquots (either 50 or 100 μL) of a GdnHCl denaturant solution (7.79 M, pH 8.3, 100 mM Tris-HCl, 1 mM EDTA) were added into the optical cell sequentially. The concentration of the stock GdnHCl solution was determined using a Bausch and Lomb refractometer. The absorbance of the protein was determined 5 min after the addition of each aliquot of denaturant. The absorbance data were collected continually for 1 min and averaged. The data were corrected for buffer absorbance and for protein dilution prior to analysis. Experiments with two RNase A mutants, [C40S/C95S] RNase A and [C65S/C72S] RNase A, obtained from a previous study (*20*), were carried out under similar conditions.

Estimation of Thermodynamic Parameters of Two AEMTS-Blocked Des Species of RNase B Intermediates and Three-Disulfide-Containing RNase A Mutant Analogues from Their Chemical Denaturation Curves. For the analysis of the thermodynamic parameters, we assumed a two-state model, which was used to fit the chemical denaturation profile of RNase A and its mutants obtained under similar conditions (*27*−*30*). This assumption is valid since no intermediates were detected in the denaturation curve of RNase B intermediates and two RNase A mutants. The fraction of folded protein at each denaturant concentration was obtained as described previously (*29*). The midpoint of the transition curves was obtained by fitting the fraction of folded species against denaturant concentration with a sigmoidal function. The standard free energy of conformational unfolding of a protein, $\Delta G°$, at different denaturant concentrations, was calculated by the following equation.

$$\Delta G° = -RT \ln K_D = -RT \ln \frac{f_D}{f_N} \qquad (1)$$

where K_D is the unfolding equilibrium constant, f_D and f_N are the fractions of denatured and folded AEMTS-blocked species for RNase B and mutants for RNase A, respectively, R is the universal gas constant, and T is the absolute

temperature. By extrapolation of the chemical denaturation curve within the linear region of folded protein to zero denaturant concentration according to eq 2, the standard free energy of unfolding in aqueous buffer can be obtained at the experimental temperature (*28*, *31*, *32*). The standard free energy of unfolding ($\Delta G°$) provides a measure of the stability of the protein under the given conditions.

$$\Delta G° = \Delta G°_{H_2O} - mC_{GdnHCl} \quad (2)$$

where *m* is a measure of the dependence of the standard free energy on the denaturant concentration and C_{GdnHCl} is the GdnHCl concentration.

Preparation of the Unstructured Isomer (3S) Precursor of the Des Species (3S).* To study the rate of formation of the structured des species (3S*) from its unstructured precursor isomers, the unblocked 3S ensemble must be obtained. The unblocked 3S ensemble was prepared as follows.

During the oxidative folding of RNase B, a reduction pulse was applied, and the native protein, two unblocked des species, and fully reduced unblocked protein were separated by reversed-phase HPLC. These species were then collected separately and lyophilized. The two unblocked structured intermediates (des species) were dissolved in 200 μL of 6 M GdnHCl buffer (pH 8.3, 100 mM Tris-HCl, 1 mM EDTA, 25 °C, continuously sparged with argon to prevent air oxidation) which results in a loss of their structure and facilitates reshuffling. Incubation for 1 h at 25 °C under these conditions is sufficient to result in an equilibrium distribution of the unstructured 3S ensemble (*33*). The pH of the 3S ensemble was lowered to 3 by addition of 20 μL of glacial acetic acid, and buffer salts and GdnHCl were removed by reversed-phase HPLC, where the air oxidation is negligibly slow at pH <2. Water and organic solvents were removed by lyophilization. The identity of the unstructured 3S ensemble was verified by blocking a small amount of the lyophilized 3S material using AEMTS and comparing its elution profile (obtained by using strong cation-exchange HPLC) with that described in previous reports (*25*, *26*).

Rate of Formation of the Two Des Species from Their Unstructured 3S Ensemble. The kinetics of formation of structured three-disulfide-containing intermediates of RNase B (des species) from their unstructured precursor isomers (3S ensemble) was initiated by addition of a 4 mL of a 100 mM Tris-HCl, 1 mM EDTA buffer (pH 8.3 and 25 °C) to the lyophilized unstructured and unblocked 3S ensemble (final protein concentration of 33 μM); the mixture was continuously sparged with argon to prevent air oxidation. Aliquots of 0.5 mL samples were withdrawn at different times and subjected to a reduction pulse (5 mM DTT^{red} for 2 min) followed by AEMTS blocking of any free thiols. The pH of the sample was adjusted to 3 by addition of 20 μL of glacial acetic acid. The sample was desalted using a Hi-Trap G25 column and analyzed by cation-exchange HPLC. Application of the reduction pulse before blocking the samples with AEMTS selectively reduced all unstructured 3S isomers to the fully reduced protein, which facilitates their separation, upon AEMTS blocking, from the structured des species.

The peak areas corresponding to 3S* and the fully reduced protein (R) were integrated, and the fractional increase in

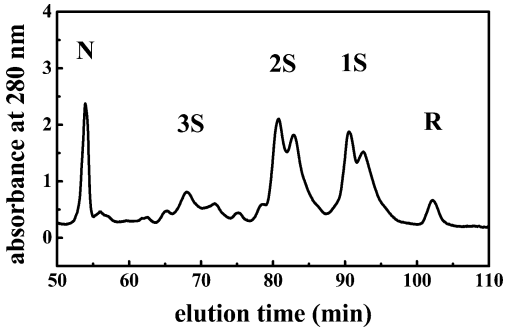

FIGURE 1: Typical cation-exchange HPLC chromatogram showing the AEMTS-blocked intermediates formed during the regeneration of RNase B (33 μM) 60 min after initiation of regeneration using 100 mM DTT^{ox} (100 mM Tris-HCl, 1 mM EDTA, pH 8.3, 25 °C).

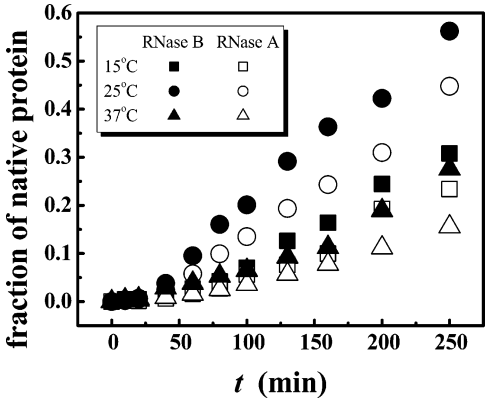

FIGURE 2: Fraction of native protein formed during the oxidative folding of RNase A and RNase B (100 mM DTT^{ox}, pH 8.3), at three different temperatures: 15, 25, and 37 °C. At each regeneration temperature, the protein concentration was 0.5 mg/mL (33 μM) in 100 mM Tris-HCl and 1 mM EDTA.

3S* was plotted as a function of time. The fractional concentration of R represents the fractional concentration of 3S since R is formed upon reduction of the 3S ensemble due to application of the reduction pulse. The data were fitted to a single-exponential function to obtain the rate constant for the formation of 3S* from 3S.

The rates of formation of the structured des species of RNase A from their unstructured isomers were also determined as described above.

RESULTS

Regeneration of RNase B. Figure 1 shows a typical HPLC chromatogram 60 min after initiation of oxidative folding (100 mM DTT^{ox}, pH 8.3, 25 °C), and blocked with AEMTS. The native protein, the 3S, 2S, and 1S ensembles, and the fully reduced protein (R) are clearly visible. Figure 2 compares the fractions of native RNase B and RNase A formed as a function of oxidative folding time at different temperatures. The sizes of the symbols indicate the standard deviations in repeat experiments. It is clear that the oxidative folding rate of RNase B is greater than that of RNase A, which is evident from the fractions of each native species formed as a function of oxidative folding time.

Results from these experiments showed that the rate of formation of the native protein (*N*) of both species is approximated well by a first-order rate equation:

$$\ln(1 - N) = -kt \quad (3)$$

Table 1: Temperature Dependence of the Rate Constants for the Regeneration of RNase A and RNase B (33 μM protein, 100 mM DTT^{ox}, 100 mM Tris-HCl, 1 mM EDTA, pH 8.3[a])

	rate constant of oxidative folding, k ($\times 10^4$ min^{-1})		
	15 °C	25 °C	37 °C
RNase A (k_A)	8.6 ± 0.6	21.5 ± 0.4[a]	6.1 ± 0.4
RNase B (k_B)	14.4 ± 1.3	33.2 ± 0.9	7.8 ± 0.3
k_B/k_A	1.7	1.5	1.3

[a] The regenerations of RNase A and RNase B were studied at pH 8.3 because we noticed a slight amount of precipitation of reduced RNase B at pH 8, which was not the case at pH 8.3. We checked our regeneration rate of RNase A with previous studies in ref *34* which had been performed at pH 8.0. We obtained a regeneration rate of (11.4 ± 0.5) × 10^{-4} min^{-1} at pH 8.0 and 25 °C which is consistent with the previously determined value of (12.5 ± 0.6) × 10^{-4} min^{-1} (*34*). This larger rate constant for RNase A (21.5 × 10^{-4} min^{-1}) at pH 8.3, compared to that at pH 8.0 (11.4 × 10^{-4} min^{-1}) and 25 °C, probably reflects the higher concentration of S^- which leads to accelerated thiol−disulfide exchange reactions at pH 8.3. It should be noted that, at the end of the regeneration, approximately 120 μM DTT^{red} would be formed by the reduction of DTT^{ox} which oxidizes protein thiols to form disulfide bonds.

where $1 - N$ is the fractional concentration of all non-native species, k represents the rate constant for the formation of the native protein, and t is the reaction time. The rate constants for the regeneration of RNase A and RNase B by 100 mM DTT^{ox} (pH 8.3) at different temperatures are shown in Table 1. The ratio of the refolding rate of RNase B to that of RNase A indicates that the glycosylated ribonuclease regenerates faster than the unglycosylated variant at each temperature that was tested, with the ratios of the rates of regeneration diminishing with an increase in temperature. The reduced rate of regeneration of both RNase A and RNase B at 37 °C reflects the decreased stability of 3S* at 37 °C compared to that at 25 °C (*20*, *34*). Since the regeneration rates of both proteins through the structured des species are decreased at 37 °C and glycosylation is unlikely to have a stabilizing effect on any unstructured intermediates, the ratio of the regeneration rates of RNase A and RNase B approaches unity ($k_B/k_A = 1.3$) with an increase in temperature.

Identity of Two Structured Intermediates on the Oxidative Folding Pathways of RNase B. A reduction pulse (5 mM DTT^{red} for 2 min) reduces any unstructured disulfide-containing species to the fully reduced protein (*26*). This technique has been applied successfully to the oxidative folding of RNase A, resulting in the detection of two structured des species at 25 °C (*26*). Figure 3 is a typical HPLC chromatogram of the AEMTS-blocked oxidative folding mixture of RNase B (100 mM DTT^{ox}, pH 8.3, 25 °C) that was subjected to a reduction pulse 200 min after initiation of regeneration. In addition to the native and fully reduced protein, only two structured species (indicated by arrows in Figure 3) are detected under the experimental conditions. It should be noted that one-disulfide-containing species (1S) tend to persist after a reduction pulse because of oxidation of the fully reduced protein (R) to its one-disulfide-containing intermediates (1S), possibly due to air oxidation.

Mass spectrometric analysis of the protein species constituting these peaks indicates that their individual masses are 152 Da greater than that of native RNase B, suggesting the addition of two AEMTS molecules per protein. Since AEMTS is thiol-specific, the addition of two AEMTS molecules is indicative of the reduction of one disulfide bond. Therefore, we conclude that each protein species lacks one disulfide bond. Furthermore, their elution positions correspond to the des [65−72] and des [40−95] intermediates of RNase B that were populated in the reductive unfolding pathway of the protein (*24*). Both of these species are oxidized to form the native molecule if the oxidative folding is allowed to continue, indicating that they are not kinetically trapped, a characteristic shared with the (unglycosylated) des [40−95] and des [65−72] intermediates of RNase A (*26*, *35*).

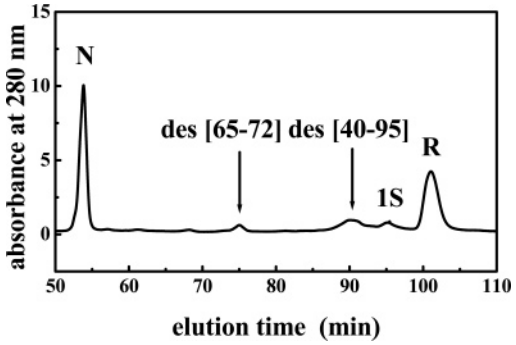

FIGURE 3: Typical HPLC chromatogram showing the AEMTS-blocked intermediates formed after the oxidative folding mixture of RNase B (33 μM) had been subjected to a reduction pulse 200 min after initiation of regeneration (100 mM Tris-HCl, 1 mM EDTA, pH 8.3, 25 °C).

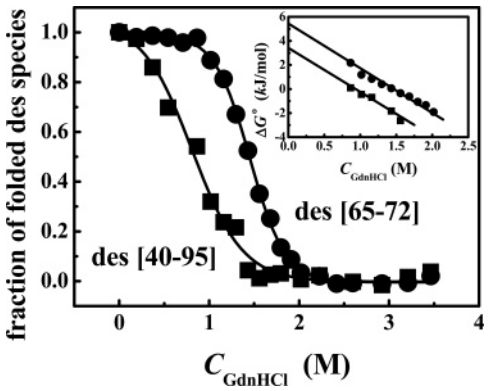

FIGURE 4: GdnHCl transition curves, and the dependence of $\Delta G°$ on the GdnHCl concentration (inset), for the AEMTS-blocked des [65−72] RNase B (●) and AEMTS-blocked des [40−95] RNase B (■) (100 mM Tris-HCl, 1 mM EDTA, pH 8.3, 25 °C).

Chemical Denaturation of AEMTS-Blocked Des [40−95] RNase B and Des [65−72] RNase B. Figure 4 shows the chemical denaturation transition curves for des [65−72] RNase B and des [40−95] RNase B blocked with AEMTS. The plots for $\Delta G°$ versus C_{GdnHCl} are linear (inset of Figure 4) and justify the use of eq 2 to obtain m and $\Delta G°_{H_2O}$. The standard free energy of unfolding, $\Delta G°_{H_2O}$, m, and midpoint $C_{1/2}$(GdnHCl) for each des species relative to its unfolded state are listed in Table 2. For comparison, the same thermodynamic parameters for the three-disulfide-containing RNase A mutants, viz., [C65S/C72S] and [C40S/C95S] RNase A, obtained under similar conditions are also listed. The data show that the two RNase B des species are slightly more stable than the three-disulfide-containing mutant analogues of RNase A, and that the des [65−72] species are more stable than the des [40−95] species for both RNase A and RNase B.

Table 2: Thermodynamic Parameters of the Three-Disulfide-Containing Intermediates of RNase A and RNase B in 100 mM Tris-HCl and 1 mM EDTA at pH 8.3 and 25 °C

protein[a]	$\Delta G^{\circ}_{H_2O}$[b] (kcal/mol)	m[b] *(kcal mol^{-1} M^{-1})*	$C_{1/2}$(GdnHCl)[b] (M^{-1})
des [65−72] RNase B	5.4 ± 0.7	3.9 ± 0.5	1.45 ± 0.01
des [40−95] RNase B	3.4 ± 0.7	3.7 ± 0.6	0.85 ± 0.05
[C65S/C72S] RNase A	4.7 ± 0.4	3.8 ± 0.3	1.22 ± 0.01
[C40S/C95S] RNase A	2.9 ± 0.1	3.7 ± 0.1	0.77 ± 0.01

[a] Data from current experiments for two RNase B des species blocked with AEMTS and for [C65S/C72S] and [C40S/C95S] RNase A mutants at pH 8.3 and 25 °C using GdnHCl as a denaturant. [b] The parameters were obtained by the method of Santoro and Bolen (*31*). $\Delta G^{\circ}_{H_2O}$ represents the estimated standard free energy change for the folded → unfolded transition in the des species in water. m represents the first derivative of the free energy difference with respect to the GdnHCl concentration. $C_{1/2}$(GdnHCl) represents the concentration of GdnHCl at the midpoint of the transition curves. Errors are given as standard deviations.

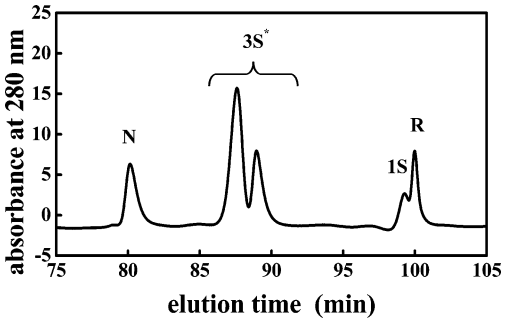

FIGURE 5: Reversed-phase HPLC chromatogram showing unblocked des species (3S*, i.e., des [65−72] and des [40−95]) obtained after applying a reduction pulse to the regeneration mixtures of RNase B. The native protein, 1S, and the fully reduced protein are also seen.

Rate of Formation of Des Species from Their Unstructured 3S Isomers (the 3S ensemble). Figure 5 is a reversed-phase HPLC chromatogram showing the separation of the unblocked des species of RNase B from the native and fully reduced protein. The formation of two pairs of structured des species (des [65−72] and des [40−95]), glycosylated for RNase B and unglycosylated for RNase A, from the unstructured 3S ensembles of RNase B and RNase A is shown in Figure 6. The curves are single-exponential fits of the experimental data for RNase B and RNase A. The rate constants for overall formation of structured des species of RNase B and RNase A at 25 °C are (2.0 ± 0.1) × 10^{-2} and (1.2 ± 0.1) × 10^{-2} min^{-1}, respectively.

DISCUSSION

Oxidative Folding Pathways of RNase B. Two structured intermediates were found to populate the oxidative folding pathway of RNase B (pH 8.3 and 25 °C) and were identified by HPLC as des [65−72] RNase B and des [40−95] RNase B. Both of them have three native disulfides (i.e., they lack the fourth disulfide). Neither species is present after prolonged oxidative folding times (i.e., 16−24 h after initiation of oxidative regeneration), indicating that they are not kinetically trapped during the oxidative folding. These results suggest that the major folding pathways of RNase B are similar to those of RNase A (Figure 7) at 25 °C (*26*), indicating that the oligosaccharide does not alter the folding pathways of bovine pancreatic ribonuclease.

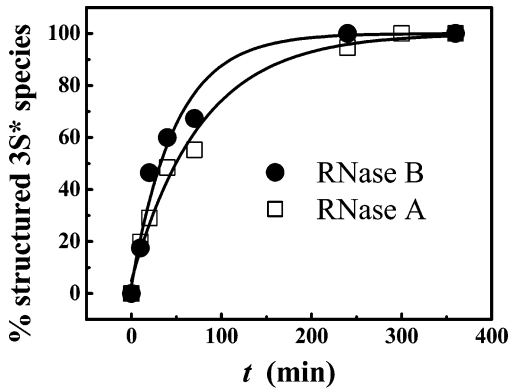

FIGURE 6: Formation of combined structured 3S* species (des [65−72] and des [40−95]) of two ribonucleases [(●) RNase B and (□) RNase A] and from its unstructured 3S ensemble (33 μM) at pH 8.3 and 25 °C in a 100 mM Tris-HCl and 1 mM EDTA buffer. The curves are single-exponential fits for the experimental data for RNase B and RNase A, respectively.

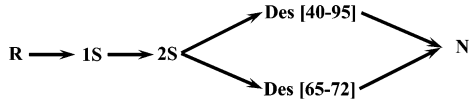

FIGURE 7: Schematic representation of oxidative folding pathways of RNase B at pH 8.3 and 25 °C.

Effect of Oligosaccharides on the Oxidative Folding Rates of RNase B. The rate-determining step in the regeneration of RNase A is the formation of structured des species from their unstructured isomers (i.e., 3S → 3S*). The formation of the native protein from its structured intermediates (3S* → N) is relatively rapid compared to the rate-determining step (*35*). Since the structured des species are involved in both the rate-determining step and the post-rate-determining step, we compared the stability and rate of formation of the des species of both variants at 25 °C and pH 8.3 in an attempt to explain the enhanced rate of regeneration of RNase B compared to that of RNase A.

The GdnHCl denaturation curves of two AEMTS-blocked RNase B des species provide information about the stability of these two species (Figure 4). The midpoint and $\Delta G^{\circ}_{H_2O}$ obtained from GdnHCl denaturation measurements are slightly higher for the RNase B intermediates than those for the RNase A intermediates (Table 2). It should be noted that the thermodynamic parameters for the three-disulfide-containing intermediates of RNase A were obtained from measurement of their cysteine-to-serine mutant analogues whereas those for the three-disulfide-containing intermediates of RNase B were obtained from their AEMTS-blocked derivatives. The slight increase in the stability of the des species of RNase B is consistent with the slight increase in the stability of native RNase B compared to that of native RNase A (*7*−*9*).

The rate constant for the formation of the des species of RNase B from their unstructured 3S ensemble [(2.0 ± 0.1) × 10^{-2} min^{-1}] is also larger than that for its oligosaccharide-free counterpart [(1.2 ± 0.1) × 10^{-2} min^{-1}], suggesting that the presence of the oligosaccharide somehow (discussed below) promotes the formation of the structured species (3S*).

Oxidative folding rates depend on the thermodynamic stabilities of structured intermediates. The higher the stability of a structured intermediate, the less chance that it will back-

reshuffle to its unstructured isomer. Thus, the more stable des intermediates of RNase B contribute to the increased regeneration rate of the protein. Furthermore, the rate of formation of a structured intermediate is also an important factor that contributes to the overall oxidative folding rate. If a structured intermediate can form very quickly from its unstructured isomers or precursors, the rate of formation of the native protein is enhanced. Our results from thermodynamic and kinetic studies of the des species of the two variants indicate that the greater thermodynamic stability and increased rate of formation of the structured intermediates of RNase B compared to those of RNase A are responsible for the enhanced rate of regeneration of RNase B compared to that of RNase A.

The increase in the stability of AEMTS-blocked des [40−95] and des [65−72] RNase B relative to that of des [40−95] and des [65−72] RNase A is consistent with the decreased amide−proton deuterium exchange rates for a large number of residues of native RNase B compared to RNase A (*6*). The protection of amide protons has been attributed to steric hindrance between the sugar moiety and the protein which reduces solvent accessibility and stabilizes the protein by approximately 1.2 kcal/mol (*6*).

CONCLUSION

These studies concerning the influence of oligosaccharides on the oxidative folding pathways and regeneration rates of bovine pancreatic ribonucleases indicate that, although the oligosaccharide moiety does not alter the folding pathways of the B variant (compared to the A variant that lacks the oligosaccharide side chain), there is a definite increase in the folding rate of the glycoprotein compared to its unglycosylated variant. Thermodynamic and kinetic investigations of the stabilities and rates of formation of two key structured intermediates suggest that the underlying causes of the enhanced regeneration rate of the glycosylated protein reside in the higher thermodynamic stability and higher rate of formation of these two des species compared to those of their unglycosylated counterparts.

REFERENCES

1. Plummer, T. H., Jr., and Hirs, C. H. W. (1964) On the structure of bovine pancreatic ribonuclease B. Isolation of a glycopeptide, *J. Biol. Chem. 239*, 2530−2538.
2. Plummer, T. H., Jr., Tarentino, A., and Maley, F. (1968) The glycopeptide linkage of ribonuclease B, *J. Biol. Chem. 243*, 5158−5164.
3. Fu, D., Chen, L., and O'Neill, R. A. (1994) A detailed structural characterization of ribonuclease B oligosaccharides by ^{1}H NMR spectroscopy and mass spectrometry, *Carbohydr. Res. 261*, 173−186.
4. Wlodawer, A., Svensson, L. A., Sjölin, L., and Gilliland, G. L. (1988) Structure of phosphate-free ribonuclease A refined at 1.26 Å, *Biochemistry 27*, 2705−2717.
5. Williams, R. L., Greene, S. M., and McPherson, A. (1987) The crystal structure of ribonuclease B at 2.5 Å resolution, *J. Biol. Chem. 262*, 16020−16031.
6. Joao, H. C., and Dwek, R. A. (1993) Effects of glycosylation on protein structure and dynamics in ribonuclease B and some of its individual glycoforms, *Eur. J. Biochem. 218*, 239−244.
7. Rudd, P. M., Joao, H. C., Coghill, E., Fiten, P., Saunders, M. R., Opdenakker, G., and Dwek, R. A. (1994) Glycoforms modify the dynamic stability and functional activity of an enzyme, *Biochemistry 33*, 17−22.
8. Wormald, M. R., and Dwek, R. A. (1999) Glycoproteins: Glycan presentation and protein-fold stability, *Struct. Folding Des. 7*, R155−R160.
9. Pfeil, W. (2002) The influence of glycosylation on the thermal stability of ribonuclease, *Thermochim. Acta 382*, 169−174.
10. Schülke, R., and Schmid, F. Z. (1988) The stability of yeast invertase is not significantly influenced by glycosylation, *J. Biol. Chem. 263*, 8827−8831.
11. Marquardt, T., and Helenius, A. (1992) Misfolding and aggregation of newly synthesized proteins in the endoplasmic reticulum, *J. Cell Biol. 117*, 505−513.
12. Lis, H., and Sharon, N. (1993) Protein glycosylation. Structural and functional aspects, *Eur. J. Biochem. 218*, 1−27.
13. Rothman, J. E., and Lodish, H. F. (1977) Synchronised transmembrane insertion and glycosylation of a nascent membrane protein, *Nature 269*, 775−780.
14. Kornfeld, R., and Kornfeld, S. (1985) Assembly of asparagine-linked oligosaccharides, *Annu. Rev. Biochem. 54*, 631−664.
15. Pless, D. D., and Lennarz, W. J. (1977) Enzymatic conversion of proteins to glycoproteins, *Proc. Natl. Acad. Sci. U.S.A. 74*, 134−138.
16. Grafl, R., Lang, K., Vogl, H., and Schmid, F. X. (1987) The mechanism of folding of pancreatic ribonucleases is independent of the presence of covalently linked carbohydrate, *J. Biol. Chem. 262*, 10624−10629.
17. Yamaguchi, H., and Uchida, M. (1996) A chaperone-like function of intramolecular high-mannose chains in the oxidative refolding of bovine pancreatic RNase B, *J. Biochem. 120*, 474−477.
18. Nishimura, I., Uchida, M., Inohana, Y., Setoh, K., Daba, K., Nishimura, S., and Yamaguchi, H. (1998) Oxidative refolding of bovine pancreatic RNases A and B promoted by Asn-glycans, *J. Biochem. 123*, 516−520.
19. White, F. H., Jr. (1982) Studies on the relationship of disulfide bonds to the formation and maintenance of secondary structure in chicken egg white lysozyme, *Biochemistry 21*, 967−977.
20. Laity, J. H., Shimotakahara, S., and Scheraga, H. A. (1993) Expression of wild-type and mutant bovine pancreatic ribonuclease A in *Escherichia coli*, *Proc. Natl. Acad. Sci. U.S.A. 90*, 615−619.
21. Chiti, F., Taddei, N., Giannoni, E., van Nuland, N. A., Ramponi, G., and Dobson, C. M. (1999) Development of enzymatic activity during protein folding: Detection of a spectroscopically silent native-like intermediate of muscle acylphosphatase, *J. Biol. Chem. 274*, 20151−20158.
22. Edwin, F., and Jagannadham, M. V. (2000) Salt-induced folding of a rabbit muscle pyruvate kinase intermediate at alkaline pH, *J. Protein Chem. 19*, 361−371.
23. Narayan, M., Welker, E., and Scheraga, H. A. (2000) Oxidative folding of proteins, *Acc. Chem. Res. 33*, 805−812.
24. Xu, G., Zhai, H., Narayan, M., McLafferty, F. W., and Scheraga, H. A. (2004) Simultaneous characterization of the reductive unfolding pathways of RNase B isoforms by top-down mass spectrometry, *Chem. Biol. 11*, 517−524.
25. Rothwarf, D. M., and Scheraga, H. A. (1993) Regeneration of bovine pancreatic ribonuclease A. 1. Steady-state distribution, *Biochemistry 32*, 2671−2679.
26. Rothwarf, D. M., Li, Y.-J., and Scheraga, H. A. (1998) Regeneration of bovine pancreatic ribonuclease A: Identification of two nativelike three-disulfide intermediates involved in separate pathways, *Biochemistry 37*, 3760−3766.
27. Hermans, J., Jr., and Scheraga, H. A. (1961) Structural studies of ribonuclease. V. Reversible change of configuration, *J. Am. Chem. Soc. 83*, 3283−3292.
28. Pace, C. N. (1990) Measuring and increasing protein stability, *Trends Biotechnol. 8*, 93−98.
29. Iwaoka, M., Wedemeyer, W. J., and Scheraga, H. A. (1999) Conformational unfolding studies of three-disulfide mutants of bovine pancreatic ribonuclease A and the coupling of proline isomerization to disulfide redox reactions, *Biochemistry 38*, 2805−2815.
30. Xu, G., Narayan, M., Welker, E., and Scheraga, H. A. (2003) A novel method to determine thermal transition curves of disulfide-containing proteins and their structured folding intermediates, *Biochem. Biophys. Res. Commun. 311*, 514−517.
31. Santoro, M. M., and Bolen, D. W. (1988) Unfolding free energy changes determined by the linear extrapolation method. 1. Unfolding of phenylmethanesulfonyl α-chymotrypsin using different denaturants, *Biochemistry 27*, 8063−8068.

32. Pace, C. N., Laurents, D. V., and Thomson, J. A. (1990) pH dependence of the urea and guanidine hydrochloride denaturation of ribonuclease A and ribonuclease T1, *Biochemistry 29*, 2564−2572.
33. Narayan, M., Welker, E., and Scheraga, H. A. (2001) Development of a novel method to study the rate-determining step during protein regeneration: Application to the oxidative folding of RNase A at low temperature reveals BPTI-like kinetic traps, *J. Am. Chem. Soc. 123*, 2909−2910.
34. Rothwarf, D. M., and Scheraga, H. A. (1993) Regeneration of bovine pancreatic ribonuclease A. 4. Temperature dependence of the regeneration rate, *Biochemistry 32*, 2698−2703.
35. Rothwarf, D. M., Li, Y.-J., and Scheraga, H. A. (1998) Regeneration of bovine pancreatic ribonuclease A: Detailed kinetic analysis of two independent folding pathways, *Biochemistry 37*, 3767−3776.

BI0506932